Resonance effects in the inelastic interactions of slow electrons with alkali metal ions

A. I. Zapesochnyĭ, A. I. Imre, I. S. Aleksakhin, I. P. Zapesochnyĭ, and O. I. Zatsarinnyĭ

Institute of Nuclear Physics, Academy of Sciences of the Ukrainian SSR

(Submitted 3 December 1985)
Zh. Eksp. Teor. Fiz. **90**, 1972–1981 (June 1986)

The first studies are made of the vacuum ultraviolet radiation arising in inelastic collisions of potassium, rubidium, and cesium ions with electrons at energies 8–400 eV. The effective excitation cross sections are determined for 21 spectral lines. Their energy dependence is found to exhibit a pronounced structure, with most of the peaks having a resonance character. A detailed study is made of this structure. The entire set of data obtained in this study is attributed unambiguously to capture of the projectile electron with formation of autoionizing states of the atom or ion. The subsequent decay of these states leads to a strong selective population of the resonance levels of the ion under study, to dielectronic-recombination radiation in a narrow energy interval, and, finally, to emission of ultrasoft x rays.

1. INTRODUCTION

Experimental studies on the electron-impact excitation of ions in intersecting charged-particle beams have so far been done for a limited number of elements. Systematic research has been done only for alkaline-earth atoms.[1] The effective excitation cross sections of the resonance levels of these ions, as would be expected, are rather large (of the order of 10^{-15} cm^2). In addition, the radiation to be measured in the experiment is in the visible region of the spectrum, which is convenient from an experimental standpoint. These circumstances have made it possible to study in greater detail the energy dependence of the excitation cross sections of the resonance lines. In particular, the results confirmed the familiar laws describing the decay of the effective excitation cross sections for optically allowed and forbidden transitions at high energies.

For ions with completely or partially filled shells (e.g., ions of alkali metals and inert gases), the resonance lines fall in the difficultly accessible vacuum ultraviolet (VUV) region of the spectrum. In view of certain beam-technique peculiarities due to the limitation imposed on the density of particles in the beams by the interaction of their space charges, and also in view of the substantially smaller effective excitation cross sections of the levels of these ions, one can understand both the complexity of such studies and the almost total lack of information on experiments of this kind.

In recent years there has been growing interest in the study of the role of autoionization effects in the electron-impact excitation and ionization of ions. Isolated features on the excitation functions of certain spectral lines have been observed for the ions He^+ (Ref. 2), Li^+ (Ref. 3), and Ba^+ (Ref. 4). The authors of the studies cited interpreted these features as resonances in the ion-electron system due to interference between the twice excited states of the atom and the direct excitation of the level under study. However, the actual channels by which the excited states of the ions are populated have not been established.

Experimental and theoretical studies of the resonance structure in the excitation cross sections of the resonance levels of the Mg^+ ion have been reported recently.[5] The calculation, done by a diagonalization method with subsequent averaging over the energy spread of the electrons used in the experiment, is in good agreement with the measured data. The authors were able to identify the individual extrema in the structure with specific autoionizing states of the magnesium atom.

Ions of the alkali atoms have a completely filled outer electron shell. They typically have resonance levels that are high-lying, with components that are strongly split by the spin-orbit interaction of the electrons, and also a large number of atomic autoionizing states. Even our first experiments on the excitation of potassium, rubidium, and cesium ions in intersecting beams (see our brief communications[6–8]) revealed a sharply nonmonotonic behavior of the excitation functions of the resonance lines near the threshold. The need became clear for detailed and systematic studies of these and other inelastic processes, with a thorough analysis of the results. This is the subject of the present paper.

2. EXPERIMENTAL APPARATUS, TECHNIQUES, AND CONDITIONS

The studies were done on an apparatus having intersecting electron and ion beams (see Fig. 1a); the basic units of this apparatus are described in Ref. 1. Because the radiation of the resonance and other lines of the alkali metal ions lies in the wavelength range 50–110 nm, the high-transmission visible-region monochromator used in Ref. 1 was replaced by a vacuum monochromator.

The ion beam was produced by a source that worked by surface ionization of metal vapor on an incandescent tungsten filament. Batches of the alkali metal were loaded into the reservoir in sealed glass ampoules, which were opened in the vacuum with the aid of bimetal strips. The ion beam, having a cross section of 2.5×2.5 mm and a current 1–2 μA at an energy of 1 keV, was shaped by an ion-optical system. The ions were separated from the neutral atoms by a 90-degree electrostatic capacitor, after which the atoms that

 0038-5646/86/061155-06$04.00

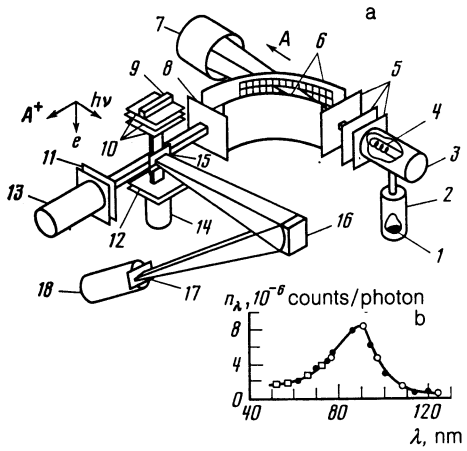

FIG. 1. (a) Schematic of experimental apparatus: 1) alkali metal, 2) heated reservoir, 3) ionization chamber, 4) tungsten cathode, 5) ion-optical system, 6) 90-degree electronic capacitor, 7) atom trap, 8) shaping slit, 9) cathode of electron gun, 10) electron-optical system, 11,12) electrodes for blocking secondary electrons, 13) ion collector, 14) electron collector, 15) entrance slit of monochromator, 16) diffraction grating, 17) exit slit, 18) radiation detector. (b) Spectral sensitivity of the apparatus versus wavelength (the filled-in points were obtained using the data of Ref. 10, the open points the data of Ref. 11, and the squares the data of Ref. 12).

had passed through a grid in the capacitor plate were precipitated on a liquid-nitrogen-cooled trap. The electron beam, of cross section 1×8 mm, was formed by a three-electrode electron gun with a heater cathode. The gun gave a well-focused electron beam with a current of 0.1–1 mA at energies ranging from 5 to 500 eV, with an energy nonuniformity of 1–3 eV at the half-height level of the distribution curve. The error in determining the electron energy was not over 0.3 eV.

The beams intersected at an angle of 90°, and the radiation of the excited ions was detected in the direction perpendicular to the plane of intersection of the beams. The vacuum was produced in the apparatus by oil-free pumps and had a value in the beam-intersection region of 10^{-8} Torr.

The spectral separation of the radiation was done with a 70-degree vacuum monochromator using the Seya-Namioka optical arrangement; this device was successfully tested in Ref. 9. Mounted in the device was a concave diffraction grating with a radius of curvature of 0.5 m and a ruling density of 1200 lines/mm. The average reciprocal linear dispersion of the device was 1.7 nm/mm. The radiation detector was a VÉU-4 secondary electron multiplier operating in the photoelectron-counting regime.

The signal from the electron-impact excitation of the ions was discriminated from the background of accompanying processes in the apparatus (electron-atom and ion-atom collisions) by the technique of modulating the two beams by rectangular phase-shifted pulses. The technique permitted discrimination of the useful signal from the total background with a minimum ratio of 1/100. To increase the detectable signal, a width of 1 mm was chosen for the entrance and exit slits of the monochromator. At this slit width the resonance lines of the K^+ ion (60.1–61.3 nm)[1)] were not resolved, nor were two of the five resonance lines of Cs^+. The effective cross section for electron-impact excitation was determined from the expression

$$\sigma=\frac{C}{I_eI_i}\frac{e^2v_ev_i}{(v_e^2+v_i^2)^{1/2}}\frac{F}{\eta_\lambda}, \tag{1}$$

where C is the measured signal in counts/sec, I_e and I_i are the currents of the electron and ion beams, v_e and v_i are the electron and ion velocities, e is the electron charge, η_λ is the spectral sensitivity of the apparatus at wavelength λ, and F is a measure of the spatial distribution of the particles in the beams. The directly measured quantities in the experiment were the useful signal and the parameters of the beams. The geometric factor F was close to unity in our experiments. The sensitivity η_λ is difficult to determine in the VUV region for in practice the only calibrated source of VUV radiation is the synchrotron radiation of electron accelerators. The relative sensitivity of the apparatus in the spectral region 55–125 nm (see Fig. 1b was determined by the present authors using data on the effective excitation cross sections of molecular nitrogen[10,11] and atomic argon.[12] These gases were admitted into the collision chamber to a pressure of 10^{-5} Torr.

In our experiments the signal from the electron-impact excitation of the ion varied between 0.1 and 1 pulse/sec, and the signal-to-noise ratio varied from 1/1 in the near-threshold energy region to 1/50 at an energy of 400 eV. The signal was accumulated in series of 7–10 measurements with exposure times of up to 1000 sec. Each experimental point is the result of an averaging of the data from one series of measurements. Because of the small value of the signal and the dominance of the background, the mean square error of the relative measurements was 10–40%. The main contribution to the uncertainty of the measurements was from random error due to the statistical nature of the measured signal.

III. TECHNIQUES USED IN THE THEORETICAL CALCULATIONS AND FOR DETERMINING THE EFFECTIVE EXCITATION CROSS SECTIONS OF IONS

The absolute values of the excitation cross sections were determined by theoretical calculations. The calculations for the ions K^+, Rb^+, and Cs^+ were done in the Coulomb-Born approximation on an ES-1020 computer by the technique described in Ref. 13. The effective cross sections for excitation from the ground state to the resonance states $np^5(n+1)s$ were determined from the expression

$$\sigma=(\pi a_0^2)g\frac{8}{3E}\max(l_0l_1)\sum_{l'l}\max(l'l)\times\left[\int_0^\infty F_{l'}F_l\left(\int_0^\infty P_0(r')P_1(r_1)\frac{r_<}{r_>^2}dr'\right)dr\right], \tag{2}$$

where l_0, l, l_1, l' are the orbital angular momenta of the target electron and projectile electron, respectively, in the initial and final states, P_0, P_1, F_l, and $F_{l'}$ are the radial parts of the wave functions of the respective electrons, E is the energy of the projectile electron in rydbergs, a_0 is the Bohr radius, and g is a numerical coefficient which depends on the type of coupling. The function F_l was found by numerical integration of the standard equation, and the functions $P(r)$ were determined by Hartree-Fock calculations done with a se-

miempirical fitting of the core potential obtained using the data of Ref. 14.

We see from Eq. (2) that the calculated effective excitation cross section depends on the type of coupling. The applicability of *jl* coupling for describing the resonance levels of the Rb^+ ion was studied in Ref. 15. It was established that *jl* coupling in almost pure form is realized only for the lowest level $5s[3/2]_1^0$, while the coupling for the levels of the np^5nd configuration is of an intermediate type. Therefore, the $4p^5(^2P_{3/2}^0)5s\,[3/2]_1^0$ level of Rb^+ was chosen as the most suitable for normalizing the experimental curve. The normalization was done for the corresponding 74.1-nm resonance line at an energy of 400 eV, which amounts to approximately 24 times the energy of the excitation threshold (where the reliability of the Coulomb-Born approximation is assured). By substituting the calculated value of the cross section, $1.9\cdot10^{-17}$ cm^2, into Eq. (1), we obtain the value of the absolute spectral sensitivity of the apparatus: $4\cdot10^{-6}$ pulses/photon (at a single point) at a wavelength of 74.1 nm. In this way we calibrated the spectral sensitivity curve of the apparatus over the range 50–125 nm (see Fig. 1b). This in turn enabled us to determine the values of the effective excitation cross sections of the remaining resonance lines of the ions K^+, Rb^+, and Cs^+.

According to our estimates, such a method of determining the effective excitation cross sections has an error of ~100%. This error includes the error in measuring the excitation function in the investigated energy region (40%), the error in determining the relative spectral sensitivity of the apparatus (40%), the imprecision of the calculations (10%), and the error in the normalization at the energy of 400 eV (10%).

IV. RESULTS AND DISCUSSION

1. In a series of lengthy experiments we studied the spectra of VUV radiation emitted in collisions of slow electrons with potassium, rubidium, and cesium ions. We made a detailed study of the excitation functions of 21 spectral lines and determined their effective excitation cross sections over a wide range of electron-beam energies (from the threshold of the process up to 400 eV).

All the sectral lines can be arbitrarily divided into three classes according to their excitation thresholds. To the first class belong lines whose excitation thresholds are lower than the excitation thresholds of the resonance levels of the ions (these are the 72.3 and 75.5 nm lines of potassium, the 82.4 nm line of rubidium, and the 96.0 and 108.8 nm line of cesium). We were unable to identify these lines with the aid of the known tables of spectral lines. On the other hand, lines with these wavelengths observed in experiments on electron-atom collisions[16] were classified as radiative transitions from atomic autoionizing states. The second class includes the resonance lines of the singly-charged ions. Finally, the third class consists of lines arising at threshold energies higher than the ionization potentials of the singly-charged ions.

Figures 2–4 show the excitation functions of the lines of the three classes for each of the species studied. The excitation thresholds are indicated by arrows, the ionization boundaries of the ion are represented by the shaded regions, the rms error of the relative measurements is shown by vertical

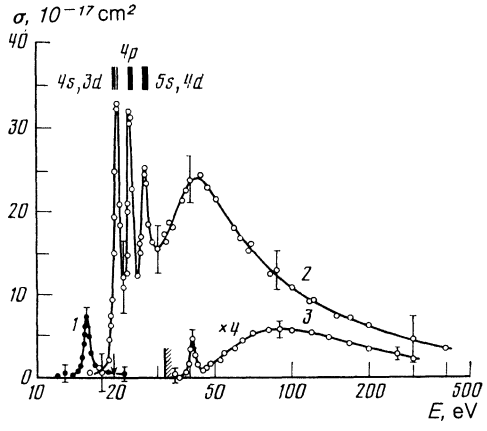

FIG. 2. Energy dependence of the effective cross section for excitation of the spectral lines of potassium: 1) 72.3 nm (K), 2) (60.1 + 60.8 + 61.3) nm (K^+), 3) 77.9 nm (K^{2+}) (×4 means that the scale on the ordinate is expanded 4 times).

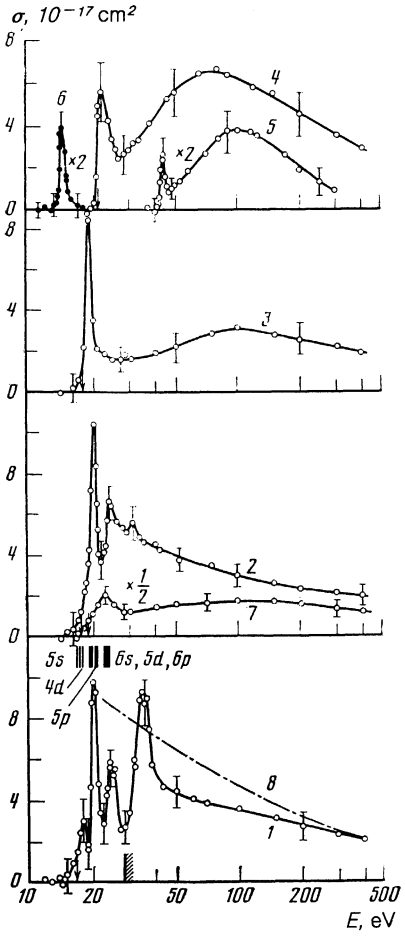

FIG. 3. Energy dependence of the effective cross sections for excitation of the spectral lines of rubidium: 1) 74.1 nm (Rb^+), 2) 71.1 nm (Rb^+), 3) 69.7 nm (Rb^+), 4) 58.9 nm (Rb^+), 5) 81.5 nm (Rb^{2+}), 6) 82.4 nm (Rb), 7) 64.4 nm (Rb^+), 8) calculated curve for the $4p^5(^2P_{3/2}^0)5s[3/2]_1^0$ level of Rb^+.

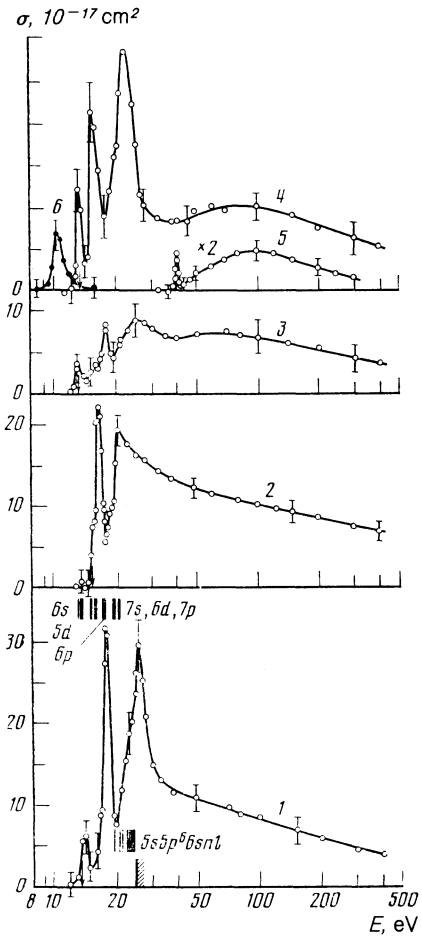

FIG. 4. Energy dependence of the effective cross sections for excitation of the spectral lines of cesium: 1) 92.7 nm (Cs^+), 2) (80.8 + 81.4) nm (Cs^+), 3) 94.1 nm (Cs^+), 4) 90.1 nm (Cs^+), 5) 87.8 nm (Cs^{2+}), 6) 96.0 nm (Cs).

bars, and the positions of the highly excited levels are indicated by hash marks. We see from the figures that the excitation functions for the lines of the different classes are substantially different, not only in terms of their threshold energies but also in their shape. One notices the presence of sharp peaks, most of which have a resonance character (their width at half-height corresponds to the spread of electron energies in the beam, 1.5–2 eV). Interestingly, the entire excitation function of the lines of the first class exhibits only a single resonance peak.

As we see from Figs. 2–4, the resonance lines of the ions are the most effectively excited, while the lines of the first and third classes have cross sections a factor of 2–3 smaller at the excitation peak. In order of magnitude, the effective excitation cross sections of the resonance lines of K^+, Rb^+, and Cs^+ are equal to 10^{-17} cm^2, and only in the near-threshold region are they 10^{-16} cm^2, which is two orders of magnitude smaller than for alkaline-earth elements. The effective excitation cross sections increase from potassium to cesium. The structure in the excitation functions lies at 1–2 times the threshold energy; the lower the resonance level lies, the richer the observed structure. Besides the narrow peaks near the excitation threshold of the resonance lines originating from the levels of the d configuration, there is a broad, gentle maximum in the energy region 50–100 eV. Starting at an energy of 150 eV, the excitation cross section of the resonance lines falls off as $E^{-1}\ln E$, as is typical for optically allowed transitions.

The obtained energy dependence of the effective excitation cross sections evidently reflects the process of potential excitation of the resonance lines, starting at about 10 times the threshold energy. In the region below 100 eV, and expecially from the threshold to the ionization boundary, the measured excitation functions are complicated by the presence of additional channels for the population of the resonance levels of the ions. For this reason it is hard to judge the value of the cross section at and near the excitation threshold.[2)]

2. Let us now consider in more detail the structure on the energy curves of the effective excitation cross sections of the resonance lines, i.e., the lines of the second class. It is seen from Figs. 2–4 that their excitation functions exhibit two types of peaks: 1) peaks with a width approximately equal to the energy spread of the beam electrons (1.5–2 eV), and 2) peaks which are several times wider. Comparison of the shape and width of the type-1 peaks with the electron energy distribution function reveals a similarity between them. This confirms the resonance nature of the observed peaks on the excitation function. Therefore, we assume that the projectile electrons are captured by ions, forming short-lived atomic autoionizing states. Alkali elements have a large number of autoionization states, which, owing to the spin-orbit splitting, converge to two different limits: $np^5{}^2P_{3/2}{}^0$ and $np^5{}^2P_{1/2}{}^0$. Some of the autoionization states are metastable with respect to autoionization, and they undergo radiative decay.[16]

The subsequent electronic decay of the autoionizing states to excited levels of the ion also leads to the appearance of resonance on the excitation function. In the case of alkaline earth ions this decay is accompanied by a change in the principal quantum number n_1 or orbital quantum number l_1 of the excited electron, as was observed in Ref. 5. In alkali elements, some of the autoionizing states can decay without a change in the quantum numbers n_1 and l_1 of the excited electrons. A study of the photoabsorption spectra of the rare earth elements has established[17] that for atoms with large (several eV) spin-orbit splittings of the excited levels, the Coster-Kronig process occurs efficiently. It is natural to assume that the decay of the autoionizing states of alkali atoms by the Coster-Kronig effect will lead not only to the direct population of the resonance levels of the ion but also to their cascade population:

$$A^+(np^6)+e\to A^{**}[np^5(^2P_{1/2})n_1l_1n_2l_2]\to A^{+*}[np^5(^2P_{1/2})n_1l_1]+\tilde{e}, \quad (3)$$

where $\tilde{e}$ is the ejected electron.

Comparison of the energy positions of the peaks of the first type on the excitation function with the energies of the excited levels of the ions under study has shown a definite correlation (see Figs. 2–5). The correlation is as follows: the first peak on the excitation functions of the (60.1 + 60.8 + 61.3) nm line of K^+, the 74.1 nm line of

Rb^+, and the 94.1, 92.7, and 90.1 nm lines of Cs^+ arises as a result of the process in Eq. (3), with $n_1 l_1 = (n+1)s$ or nd. The second peak on the excitation functions of the (60.1 + 60.8 + 61.3) nm line of K^+, the 74.1 nm line of Rb^+, and the 92.7 and 90.1 nm lines of Cs^+ and the analogous first peak (the dominant peak) on the excitation functions of the 69.7 nm line of Rb^+ and the (8018 + 81.4) nm line of Cs^+ arise when even when only the radiative cascades from the levels of the configuration $np^5(^2P_{3/2})(n+1)p$ are taken into account. The third peak on the excitation functions of the (60.1 + 60.8 + 61.3) nm line of K^+ and the 74.1 nm line of Rb^+ and the corresponding first peak on the excitation functions of the 64.4 and 58.9 nm lines of Rb^+ are the result of the total contribution of the group of autoionizing states which converge to highly excited levels, i.e., for which $n_1 > n+1$. This is most clearly seen for the K^+ ion.[6] The relative contribution of the autoionizing states to the excitation cross section changes as we go from one resonance to another. The difference in the excitation functions for levels of the same type in Rb^+ and Cs^+ is explained by the change in their relative position (see Figs. 3 and 4). The "omission" of the two levels of the configuration $5p^5(^2P_{3/2})5d$ leads to a substantial change in the form of the corresponding resonance lines (the 69.7 nm line of Rb^+ and the 94.1 nm line of Cs^+, the 58.9 nm line of Rb^+ and the 90.1 nm line of Cs^+).

The second type of peaks on the excitation functions, having widths of 5–10 eV, lie near the ionization boundary of the ion and can be attributed to the decay of atomic and ionic autoionizing states of the types $A^{**}(nsnp^6 n_1 l_1 n_2 l_2)$ and $A^{+**}(nsnp^6 n_1 l_1)$, respectively (see Fig. 5). The atomic autoionizing states are formed upon the capture of the projectile electron with a simultaneous excitation of an electron from the s^2 subshell, while the ionic autoionizing states are formed upon only the excitation of an s electron. The energies of these states are found in the literature only for the cesium atom. According to calculations,[18] the atomic autoionizing states of the type $5s5p^6 6s n_1 l_1$ lie in the energy interval 19.5–24.5 eV, and the limit of this series is the ionic autoionizing state $5s5p^6 6s$. Since this state lies below the ionization boundary $5s^2 5p^5 {}^2P_{3/2}{}^0$, it can decay only by a radiative pathway to the resonance levels $5s^2 5p^5(^2P_{3/2})6s[3/2]_1{}^0$ and $5s^2 5p^5(^2P_{1/2})6s[1/2]_1{}^0$ of the ion. The presence of a peak of the second type on the excitation function of the 90.1 nm line of Cs^+ from the level $5p^5(^2P_{3/2})5d[1/2]_1{}^0$ can be interpreted in an analogous way.

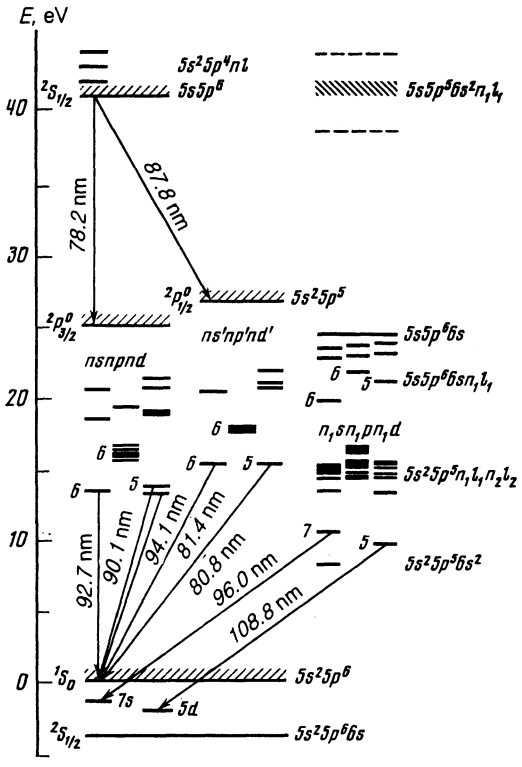

FIG. 5. Energy level scheme of cesium.

3. The spectral lines of the first class arise in the capture of the projectile electron by an alkali-metal ion with the formation of twice excited states which are metastable with respect to Coulomb autoionization and decay by a radiative pathway:

$$A^+(np^6)+e \rightarrow A^{**}(np^5 n_1 l_1 n_2 l_2) \rightarrow A^*(np^6 n_2 l_2)+h\nu. \qquad (4)$$

This kind of inelastic interaction between an electron and a positive ion is called dielectronic recombination. The radiation accompanying this process is possible only in an extremely narrow region of projectile electron energies (therefore, the excitation function of the radiation is confined to a single resonance peak).[19]

We see from Figs. 2–4 that the effective cross sections for dielectric recombination are comparable in order of magnitude with the cross section for excitation of the resonance levels of the ions K^+, Rb^+, and Cs^+. This attests to the comparatively high efficiency of the capture of the projectile electrons by ions having a filled outer shell np^6.

The identification of the upper and lower levels of the spectral lines of the first class in Ref. 16 was made by the authors on the basis of a careful analysis of the experimental and theoretical results. Here one must not fail to take into account the possibility of the cascade population of the upper levels of the observed spectral lines through radiative transitions between autoionizing states. Such transitions have been observed experimentally for the lithium atom.[20]

4. The spectral lines of the third class are formed as a result of the process of s ionization of the ions:

$$A^+(ns^2np^6)+e \rightarrow A^{2+*}(nsnp^6)+2e \rightarrow A^{2+}(ns^2np^5)+h\nu+2e. \qquad (5)$$

The radiation arising in this process is x radiation with a doublet structure (M_1–M_{23}, N_1–N_{23}, and O_1–O_{23} for the ions K^+, Rb^+, and Cs^+, respectively).[21]

A distinctive feature of the excitation function of these lines is the presence of a resonance near the threshold of the process. Our analysis permits a clear interpretation of this effect. The electronic capture of the projectile electrons is accompanied in this case by the simultaneous excitation of two electrons from the s^2 and p^6 shells:

$$A^+(ns^2np^6)+e \rightarrow A^{**}[nsnp^5(n+1)s^2 n_1 l_1]. \qquad (6)$$

There is no information in the literature concerning the binding energies of these autoionizing states. However, states of the type $nsnp^5n_1l_1n_2l_2$ have been observed in the photoabsorption spectrum of argon[22] and have also been detected in a study of the electron-impact ionization of the argon atom.[23]

Estimates of the binding energy show that the projectile electron energy corresponding to the threshold for s ionization is sufficient for excitation of two electrons. A typical scheme for autoionizing states of this type is shown in Fig. 5. It is seen that some of the autoionizing states lie above the threshold for s ionization but below the energy of the first excited level of the doubly-charged ion. It is these autoionizing states that can decay to the level $5s5p^6{}^2S_{1/2}$. The decay occurs in two steps. First the atomic autoionizing states decay by the most probable Coster-Kronic process:

$$A^{**}[nsnp^5(^1P_1)(n+1)s^2n_1l_1] \rightarrow A^{+**}[nsnp^5(^3P_j)(n+1)sn_2l_2]+\tilde{e}_1, \quad (7)$$

where $\tilde{e}_1$ is the ejected slow electron. Then the ionic autoionizing states decay through Coulomb autoionization:

$$A^{+**}[nsnp^5(n+1)sn_2l_2] \rightarrow \begin{array}{l} A^{2+*}(nsnp^6)+e_2, \\ \downarrow \\ A^{2+}(ns^2np^5)+h\nu, \end{array} \quad (8)$$

where e_2 is the ejected electron. Thus an additional resonance channel for population of the state $nsnp^6{}^2S_{1/2}$ of the doubly-charged ions arises that does not involve the detachment of an s electron.

5. CONCLUSION

Our studies have shown that the spectroscopic technique in combination with the intersecting-beams method is extremely promising for studying resonance processes in inelastic collisions of electrons with ions. The results indicate that an important role is played by the capture of the projectile electrons by alkali-metal ions, with the formation of short-lived superexcited (autoionizing) states of the neutral atoms and ions. For ions with an appreciable spin-orbit splitting of the levels, the decay of the autoionizing states formed in the electron capture occurs efficiently through the Coster-Kroning effect. In the near-threshold energy region the population of the excited levels of the alkali-metal ions occurs predominantly on account of resonance processes.

[1)]Because of the low spectral sensitivity of the apparatus in the region below 50 nm, it was not possible to study the resonance lines of the Na^+ ion (37.2 and 37.6 nm).

[2)]We note that the presence of a signal below the threshold for excitation of the resonance level is due to the nonuniform energy of the beam electrons.

[1]I. P. Zapesochnyĭ, V. A. Kel'man, A. I. Imre, A. I. Dashchenko, and F. F. Danch, Zh. Eksp. Teor. Fiz. **69**, 1948 (1975) [Sov. Phys. JETP **42**, 989 (1975)].
[2]K. T. Dolder and B. Peart, J. Phys. B **6**, 2415 (1973).
[3]W. T. Rogers, J. Ø. Olsen, and G. H. Dunn, Phys. Rev. A **18**, 1353 (1978).
[4]D. H. Crandall, P. O. Taylor, and G. H. Dunn, Phys. Rev. A **10**, 141 (1974).
[5]I. P. Zapesochnyĭ, A. I. Dashchenko, V. I. Frontov, *et al.*, Pis'ma Zh. Eksp. Teor. Fiz. **39**, 45 (1984) [JETP Lett. **39**, 51 (1984)].
[6]A. I. Zapesochnyĭ, I. S. Aleksakhin, I. P. Zapesochnyĭ, and A. I. Imre, Pis'ma Zh. Eksp. Teor. Fiz. **29**, 231 (1978) [JETP Lett. **29**, 207 (1978)].
[7]A. I. Imre, A. I. Zapesochnyĭ, V. M. Tsil'o, and M. V. Rishko, Ukr. Fiz. Zh. **25**, 1231 (1980).
[8]A. I. Zapesochnyĭ, Zh. Tekh. Fiz. **50**, 659 (1980) [Sov. Phys. Tech. Fiz. **25**, 399 (1980)].
[9]I. S. Aleksakhin, V. S. Vukstich, and I. P. Zapesochnyĭ, Zh. Eksp. Teor. Fiz. **66**, 1973 (1974) [Sov. Phys. JETP **39**, 971 (1974)].
[10]W. Sroka, Z. Naturforsch. Teil A **24**, 398 (1969).
[11]J. F. Aarts and F. J. De Heer, Physica (Utrecht) **52**, 45 (1971).
[12]K. H. Tan and A. McKonkey, Phys. Rev. A **10**, 1212 (1974).
[13]L. A. Vaĭnshteĭn, I. I. Sobel'man, and E. A. Yukov, Secheniya Vozbuzhdeniya Atomov i Ionov Elektronami [Cross Sections for the Excitation of Atoms and Ions by Electrons], Nauka, Moscow (1973).
[14]E. Clementi and G. Roetti, Atomic Data and Nuclear Data Tables **14**, 177 (1974).
[15]J. Reader and G. Epstein, J. Opt. Soc. Am. **163**, 1153 (1973).
[16]I. S. Aleksakhin, G. G. Bogachev, I. P. Zapesochnyĭ, and S. Yu. Ugrin, Zh. Eksp. Teor. Fiz. **80**, 2187 (1981) [Sov. Phys. JETP **53**, 1140 (1981)].
[17]D. H. Tracy, Proc. R. Soc. London Ser. A**357**, 485 (1977).
[18]R. K. Peterkop, Izv. Akad. Nauk Latv. SSR Ser. Fiz. Nauk **1**, 3 (1976).
[19]I. S. Aleksakhin, A. I. Zapesochnyĭ, and A. I. Imre, Pis'ma Zh. Eksp. Teor. Fiz. **28**, 576 (1978) [JETP Lett. **28**, 531 (1978)].
[20]I. S. Aleksakhin, G. G. Bogachev, I. P. Zapesochnyĭ, and S. Yu. Ugrin, Pis'ma Zh. Eksp. Teor. Fiz. **40**, 459 (1984) [JETP Lett. **40**, 1287 (1984)].
[21]I. S. Aleksakhin, A. I. Zapesochnyĭ, and A. I. Imre, Pis'ma Zh. Eksp. Teor. Fiz. **31**, 42 (1980) [JETP Lett. **31**, 38 (1980)].
[22]R. P. Madden, D. L. Ederer, and K. Codling, Phys. Rev. **177**, 136 (1969).
[23]P. Marmet, E. Bolduc, and I. I. Quemener, Can. J. Phys. **53**, 2438 (1975).

Translated by Steve Torstveit